Chem Biol Drug Des 2009; **73:** 355–364

Research Letter

doi: 10.1111/j.1747-0285.2009.00781.x

Histone Deacetylase Inhibition Activity and Molecular Docking of (*E*)-Resveratrol: Its Therapeutic Potential in Spinal Muscular Atrophy

Didem Dayangaç-Erden[1,*], Gamze Bora[1], Peruze Ayhan[2], Çetin Kocaefe[1], Sevim Dalkara[3], Kemal Yelekçi[4], Ayhan S. Demir[2] and Hayat Erdem-Yurter[1]

[1]*Department of Medical Biology, Faculty of Medicine, Hacettepe University, Ankara, Turkey*
[2]*Department of Chemistry, Middle East Technical University, Ankara, Turkey*
[3]*Department of Pharmaceutical Chemistry, Faculty of Pharmacy, Hacettepe University, Ankara, Turkey*
[4]*Department of Statistics and Computer Sciences, Faculty of Arts and Science, Kadir Has University, Istanbul, Turkey*
**Corresponding author: Dr Didem Dayangaç-Erden, didayan@hacettepe.edu.tr*

Spinal muscular atrophy is an autosomal recessive motor neuron disease that is caused by mutation of the survival motor neuron gene (*SMN1*) but all patients retain a nearly identical copy, *SMN2*. The disease severity correlates inversely with increased *SMN2* copy. Currently, the most promising therapeutic strategy for spinal muscular atrophy is induction of *SMN2* gene expression by histone deacetylase inhibitors. Polyphenols are known for protection against oxidative stress and degenerative diseases. Among our candidate prodrug library, we found that (*E*)-resveratrol, which is one of the polyphenolic compounds, inhibited histone deacetylase activity in a concentration-dependent manner and half-maximum inhibition was observed at 650 μM. Molecular docking studies showed that (*E*)-resveratrol had more favorable free energy of binding (−9.09 kcal/mol) and inhibition constant values (0.219 μM) than known inhibitors. To evaluate the effect of (*E*)-resveratrol on SMN2 expression, spinal muscular atrophy type I fibroblast cell lines was treated with (*E*)-resveratrol. The level of full-length *SMN2* mRNA and protein showed 1.2- to 1.3-fold increase after treatment with 100 μM (*E*)-resveratrol in only one cell line. These results indicate that response to (*E*)-resveratrol treatment is variable among cell lines. This data demonstrate a novel activity of (*E*)-resveratrol and that it could be a promising candidate for the treatment of spinal muscular atrophy.

Key words: (*E*)-resveratrol, molecular docking, *SMN2*, spinal muscular atrophy

Received 7 September 2008, revised and accepted for publication 1 January 2009

Proximal spinal muscular atrophy (SMA) is a neuromuscular disorder caused by the degeneration of alpha motor neurons in the anterior horns of the spinal cord. Based on age of onset and severity of the disease, SMA patients are classified as type I, II or III (1,2). All three forms of SMA are caused by homozygous deletion of the survival motor neuron 1 (*SMN1*) gene (3–5). A nearly identical copy, *SMN2*, is retained in all SMA patients and the number of the copies modulates the severity of the disease. However, the expressed amount of the SMN protein from *SMN2* does not provide adequate protection from SMA (6). The *SMN1* and *SMN2* gene differ functionally by a single nucleotide change in exon 7 that alters the activity of an exonic splice enhancer. *SMN1* produces a majority of full-length SMN transcript (FL-*SMN1*), whereas *SMN2* generates mostly an isoform lacking exon 7 (*SMN2*Δ7). Truncated Δ7-SMN proteins are reduced in their ability to self-oligomerize, which is essential for proper SMN function (7). There is a tight correlation between the clinical severity of SMA, the number of *SMN2* copies and the SMN protein level (8). The SMN protein plays an important role in the assembly and regeneration of small nuclear ribonucleoproteins, nuclear pre-mRNA splicing and axonal transport of RNA (9–11).

The disease-modifying property of the *SMN2* gene has been verified in mouse models, confirming *SMN2* as a therapeutic target (12). Several studies have demonstrated that fatty acids (13–16), benzamide (17) and hydroxamic acids (18,19) which inhibit histone deacetylases (HDAC), increase full-length *SMN2* (FL-*SMN2*) levels *in vitro* by transcriptional activation and/or by modulation of the *SMN2* splicing pattern. Histone deacetylases and histone acetyl transferases are involved in controlling the acetylation state of histones. Histone acetylation promotes gene transcription by relaxing chromatin structure and facilitating access to DNA by the transcriptional machinery, whereas histone deacetylation promotes a condensed chromatin state and transcriptional repression (20). Among 11 HDAC enzymes, HDAC 8 was the first human HDAC whose three-dimensional and X-ray crystal structure was described (21) and it is widely used in molecular docking studies to elucidate the binding properties of HDAC inhibitors (22). Some of these inhibitors are currently being studied in the clinical trials of SMA patients (23–25).

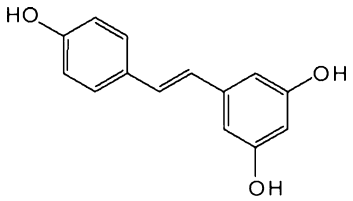

Figure 1: Chemical structure of (*E*)-resveratrol.

The search for novel and effective SMA therapeutic agents has led to the identification of various naturally occurring compounds. Polyphenols which possess more than one phenol unit per molecule are plant-originated compounds. They are famous for their antioxidant properties and health benefits (26). Of these polyphenolic compounds, (*E*)-resveratrol (3,5,4′-trihydroxy-*trans*-stilbene) which belongs to the stilbene class, is a naturally occurring compound and is part of the human diet (27). The chemical structure of (*E*)-resveratrol is illustrated in Figure 1.

(*E*)-resveratrol has been shown to have many biological properties, such as cardiovascular-protective, cancer-chemopreventive and anti-inflammatory properties including antioxidant activity (28–30). The antioxidant consumption in the diet has an important role in the protection against the development of diseases resulting from oxidative damage. Recently, oxidative stress has been shown to be involved in some aspects of SMA neurodegeneration (31). The purpose of this study was to evaluate therapeutic applications of (*E*)-resveratrol in SMA by investigating molecular docking and HDAC inhibition activity.

Materials and Methods

Molecular docking

Protein setup

The crystal structures of human histone deacetylase HDAC8 (PDB entry code: 1T64, complexed with the inhibitor trichostatin A-TSA-) (22) was obtained from the Protein Data Bank (http://www.rcsb.org). All the water and all non-interacting ions were removed together with the irreversible inhibitor of TSA.

To relieve the crystal structure tension and to make the protein available to use in the Autodock docking simulation program, all missing hydrogens/side-chain atoms were added. The obtained structure was minimized. The AUTODOCKTOOLS (version 1.5.1) (ADT) (32), graphical user interface program was employed to setup the enzymes: all hydrogen were added, Gasteiger (33) charges were calculated and non-polar hydrogen was merged to carbon atoms.

Ligand setups

The 3D structures of ligand molecules were built, optimized (PM3) level and saved in pdb format with the aid of the molecular modeling program SPARTAN[a]. The ADT package was also employed here to generate the docking input files of ligands.

AUTODOCK 3.05 (34,35) was employed for all docking calculations. The ADT generated input files were used in dockings. In all dockings, a grid box size of $80 \times 80 \times 80$ points in *x*, *y* and *z* directions was built, and because the location of the inhibitor in the complex was known, the maps were centered on Zn atom in the catalytic site of the protein. A grid spacing of 0.375 Å (approximately one-forth of the length of a carbon–carbon covalent bond) and a distance-dependent function of the dielectric constant were used for the calculation of the energetic map. Ten runs were generated by using Lamarckian genetic algorithm searches. Default settings were used with an initial population of 50 randomly placed individuals, a maximum number of 2.5×10^7 energy evaluations, and a maximum number of 2.7×10^4 generations. A mutation rate of 0.02 and a crossover rate of 0.8 were chosen. Results differing by less than 0.5 Å in positional root mean square deviation were clustered together and the results of the most favorable free energy of binding were selected as the resultant complex structures. All calculations were carried out on an IBM Intellistation Z Pro Intel Xeon 5160 machine (IBM, Armonk, NY, USA) with an Intel core duo processor at 2×3 GHz with 4 GB of RAM. The resultant structure files were analyzed using ADT and visual molecular dynamics (VMD) (36) visualization programs.

HDAC inhibition activity screening

Histone deacetylase inhibition activity of (*E*)-resveratrol was investigated by a fluorimetric assay (BioVision™, Heidelberg, Germany). The inhibitor candidate was mixed with HeLa nuclear extract which contains variety of HDAC enzymes and has HDAC activity. HDAC fluorometric substrate [Boc-Lys(Ac)-AMC], which comprises an acetylated side-chain was added to the inhibitor and HeLa nuclear extract mixture. Deacetylation sensitized the substrate and treatment with the lysine developer produced the fluorophore. The resulting fluorescence was measured with a fluorescence plate reader (Molecular Devices Spectramax M2, Sunnyvale, CA, USA) at excitation 350 nm and emission 440 nm. Decreasing fluorescence signal showed HDAC activity.

Dose–response curve following (*E*)-resveratrol treatment was analyzed by non-linear regression analysis. Determination of the IC_{50} value for the inhibition of HDAC activity was performed by using GRAPHPAD PRISM 4.0 software (San Diego, CA, USA).

Cell culture and (*E*)-resveratrol treatment

Human fibroblast cell lines from 3-year-old (GM03813; Coriell Cell Repository) and 2-year-old (GM09677; Coriell Cell Repository) SMA type I patients with two copies of the *SMN2* gene were maintained. 5×10^5 cells were transferred into 6-cm dishes using DMEM medium supplemented with 10% FCS, 1% penicillin/streptomycin, 1% L-glutamine (Biochrom, Berlin, Germany) and were incubated at 37 °C with 5% CO_2. (*E*)-resveratrol (Sigma, St Louis, MO, USA) was dissolved in DMSO (Applichem, Darmstadt, Germany) before treatment and added to the cell medium for a final concentration of 30, 100 and 300 μM. A range of time periods (6, 12, 24, 48 and 72 h) were used to determine the optimal treatment duration. Every 24 h, (*E*)-resveratrol was repetitively administered to prevent decline of the transcript level. For each experiment, complete medium was added to one of the dishes, serving as a control.

Quantitative real-time PCR of transcript levels

Total RNA was extracted from cell culture dishes using the RNeasy Mini Kit (Qiagen, Valencia, CA, USA) according to the manufacturer's protocols. The quantity and purity of isolated RNA was assessed by the NanoDrop ND-1000 Spectrophotometer (Thermo Scientific, Wilmington, DE, USA). Four hundred and fifty nanograms of each RNA sample were converted to cDNA using Quantitect RT (Qiagen). Aliquots of 25 mL quantitative PCR reactions were run in triplicate using the iQ5 Real-Time PCR Detection System (Bio-Rad Lab, Hercules, CA, USA). Primers were chosen to bind in SMN exon 6 (5′-GCT GAT GCT TTG GGA AGT ATG TTA-3′) and SMN exon 7 (5′-CAC CTT CCT TCT TTT TGA TTT TGT C-3′) for amplification of FL transcripts, and the sequence of the Taqman probe localized in exon 6, was 5′-FAM-TTT CAT GGT ACA TGA GTG GCT ATC ATA CTG GCT ATT AT-TAMRA-3′. SMNΔ7 isoform was amplified using a forward primer spanning the exon 5 and 6 junction (5′-TGG ACC ACC AAT AAT TCC CC-3′) and a reverse primer spanning the exon 6 and 8 junction (5′-ATG CCA GCA TTT CCA TAT AAT AGC C-3′); the Taqman probe annealed to a sequence in exon 6 (5′-FAM-ACC ACC TCC CAT ATG TCC AGA TTC TCT TGA TG-TAMRA-3′). The level of SMN transcripts was quantified by the threshold cycle (Ct) method using GAPDH (glyceraldehyde-3-phosphate dehydrogenase) and β actin (Applied Biosystems, CA, USA) as controls. The results were normalized to untreated sample value. The experiments were repeated twice.

Western blot analysis

Cell pellets were collected after centrifugation and lysed by sonication (Sonics Vibracell, Meryin/Satigny, Switzerland) in a blending buffer (10% sodium dodecyl sulfate, 62.5 mM Tris and a mini protease inhibitor cocktail) for 20 seconds. After centrifugation, the supernatants were collected and kept frozen at −20 °C. Protein concentrations were determined by the BCA protein assay method. For Western blot analysis, protein samples were electrophoresed on 12% SDS–polyacrylamide gel. After transfer to nitrocellulose membranes (Bio-Rad) by wet blotting, immunostaining was performed using a mouse monoclonal anti-SMN antibody (BD Transduction Laboratories, 1:5000; Milan, Italy), a rabbit polyclonal anti-actin antibody (Sigma; 1:2000), a horseradish peroxidase conjugated anti-mouse and a horseradish peroxidase conjugated anti-rabbit antibody (Amersham, Princeton, NJ, USA; 1:2000). Signals were detected using ECL chemiluminescence reagent (Amersham), and the intensity was measured using SCION imaging software (Scion Image, MD, USA). Survival motor neuron and β actin ratios were determined and normalized to untreated samples. For each sample, three different Western blots were performed.

Table 1: AutoDock 3.05 estimated free energies of binding (ΔG) and inhibition constants (Ki) of (E)-resveratrol, TSA, SAHA and valproic acid

Inhibitor	Free energy of binding (ΔG,kcal/mol)	Inhibition constant (Ki, μM)
(E)-resveratrol	−9.09	0.219
TSA	−8.59	0.504
SAHA	−7.48	3.26
Valproic acid	−4.41	564

Results

Molecular docking studies

To gain insight into the binding mode, molecular docking studies were performed for (*E*)-resveratrol and known inhibitors TSA, SAHA and valproic acid. The free energy of binding and the calculated inhibition constants (K_i) for each enzyme–inhibitor complex are shown in Table 1.

It was found that (*E*)-resveratrol had more favorable free energy of binding (−9.09 kcal/mol) and inhibition constant values (0.219 μM) than known inhibitors TSA, SAHA and valproic acid.

To rationalize binding mode of enzyme ligand complexes, their structures were viewed in detail utilizing ADT and VMD. The binding mode of (*E*)-resveratrol in the HDAC8 binding cavity is shown in Figure 2. Analysis of the docking results of (*E*)-resveratrol in complex with HDAC8 revealed that the phenolic ring system of the ligand was inserted into the zinc binding cage surrounded by Asp178, Trp141, Gln263. The inhibitor snugly fits the active site cavity making various close contacts with the residues including His180, Phe208, Tyr306, Phe152, Gly151 and a zinc ion. Important interactions take place between Gln263 and one of the hydroxy group of the (*E*)-resveratrol (2.93 Å), Tyr306 side-chain hydroxy group and one of the trans double bond carbon of the (*E*)-resveratrol (2.73 Å) and Phe208 and the phenolic group of the (*E*)-resveratrol (3.20 Å).

In Figure 3A, TSA in complex with HDAC8 were shown. TSA makes three important interactions with the active side residues of HDAC8; these are, in between His143 and the hydroxamic acid carbonyl group (1.97 Å), the Tyr306 side-chain phenolic group and hydroxamic acid amide hydrogen (2.12 Å) and His180 and the carbonyl group next to benzne ring (2.15 Å). These three close interactions, as well as the complexation of the hydroxamic acid moeity with a zinc ion play role in binding. Figure 3B shows the binding mode of SAHA with HDAC8. Two important interactions in this binding, between Tyr306 (1.97 Å) and the hydroxy group of the hydroxamic acid and between His143 and carbonyl group of hydroxamic acid (1.82 Å), contribute greatly to the binding energy.

Figure 4 shows the binding interactions of valproic acid with the active side residues of the HDAC8 enzyme. The carboxylic acid group of valproic acid approaches the zinc ion as close as possible and interacts with His143 (2.58 Å) and His142 (2.67 Å). The other interacting residues are His180, Phe208, Met274, Tyr306 and Phe152.

Among the compounds tested, (*E*)-resveratrol clearly shows the highest binding capacity toward HDAC8 enzyme and the valproic acids shows the least binding ability.

Inhibition of HDAC activity by (E)-resveratrol

To investigate the total HDAC activity after the (*E*)-resveratrol treatment, we applied 20 different concentrations of (*E*)-resveratrol (10^{-11} to 10^{-2} M) to the HeLa nuclear extract. We found that

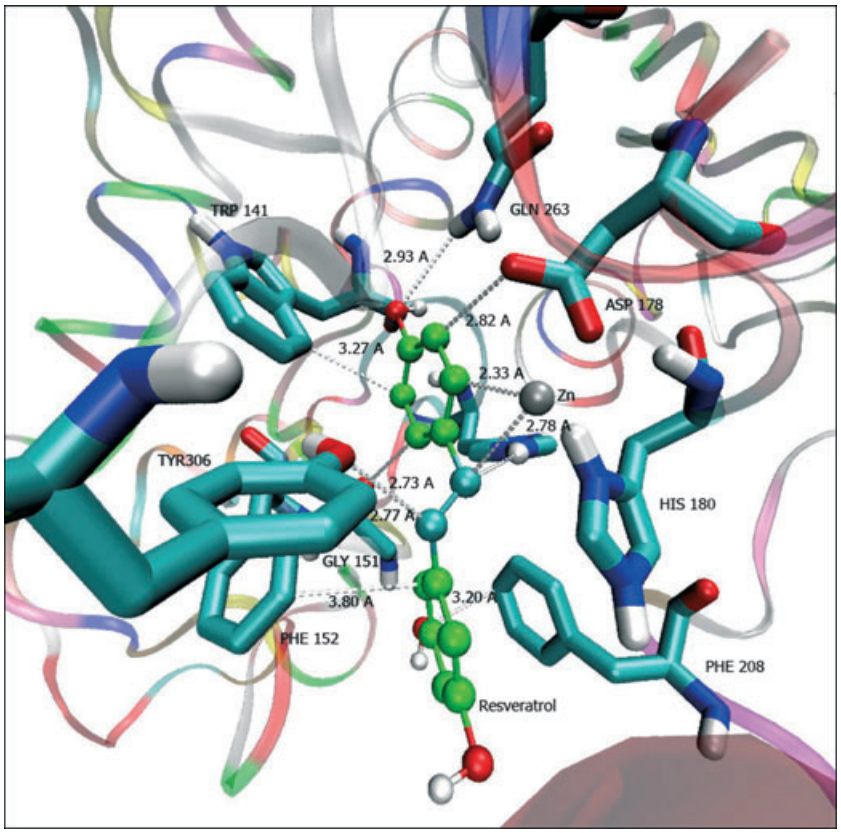

Figure 2: Docking result of (*E*)-resveratrol with HDAC8. The (*E*)-resveratrol was designated in CPK style; the important residues in the active site of the enzyme were presented by ligorice style. Part of the enzyme in the background was visualized in New Ribbon style using the VMD program.

(*E*)-resveratrol inhibited HDAC activity in a concentration-dependent manner and half-maximum inhibition (IC_{50}) was observed at 650 μM (Figure 5).

Effect of (E)-resveratrol on SMN2 gene expression

To evaluate the effect of (*E*)-resveratrol on *SMN2* gene expression and/or splicing pattern, two SMA type I fibroblast cell lines (GM03813 and GM09677) were treated with 30, 100 and 300 μM (*E*)-resveratrol for 6 h. The level of full-length *SMN2* mRNA was assessed by real-time PCR. In 3813 cell line, a significant 1.3-fold increase in full-length *SMN2* mRNA levels was found after treatment with 100 μM (*E*)-resveratrol ($p < 0.05$), whereas in 9677 cell line no increase was observed relative to untreated cultures (Figure 6).

To determine the optimal incubation period, cell lines were treated with 100 μM (*E*)-resveratrol for 6, 12 and 24 h. In 3813 cell line, a 1.3-fold increase in full-length *SMN2* mRNA and a 0.3-fold decrease in *SMN2*Δ7 mRNA levels were detected after 6 h which was statistically significant (Figure 7A). However, in 9677 cell line no increase in full-length *SMN2* mRNA levels, but a decrease in *SMN2*Δ7 mRNA levels was observed (Figure 7B).

Effect of (E)-resveratrol on SMN protein expression

To determine whether (*E*)-resveratrol could induce the SMN protein level, Western blot analyses were performed. Cells were treated with 100 μM (*E*)-resveratrol for 6, 12, 24, 48 and 72 h. Protein levels were quantified, compared with those in untreated cells and normalized to β actin which was used as a loading control. 3813 cell line reached a 1.2-fold increase in SMN protein levels at 6 h and maintained elevated levels for 12 h. In 9677 cell line, SMN protein levels remained unchanged relative to the untreated cultures between 6 and 24 h of treatment (Figure 8). At 48 h, there was a slight increase in SMN protein levels which then returned below baseline by 72 h.

Discussion

A number of potential approaches have been proposed for the treatment of SMA once the genetic basis and pathophysiology of the disease came to be understood, including activating *SMN2* gene expression, preventing *SMN2* exon 7 skipping and stabilizing SMN protein (37). The most promising strategy is to increase the levels of full-length *SMN2* mRNA and protein with HDAC inhibitors. The inhibition of HDAC allows access for transcription factors and facilitates gene activation. Histone deacetylase inhibitors are known to regulate the expression of 2–5% of genes (38); however, the mechanism by which they activate *SMN2* expression remains unknown. They may influence *SMN2* gene expression either by inducing SR proteins that modify the splicing pattern of exon 7 of *SMN2* transcripts or directly activate the *SMN2* promoter (39,40). Great efforts are currently underway for the design of more potent and less toxic candidates for the treatment of SMA.

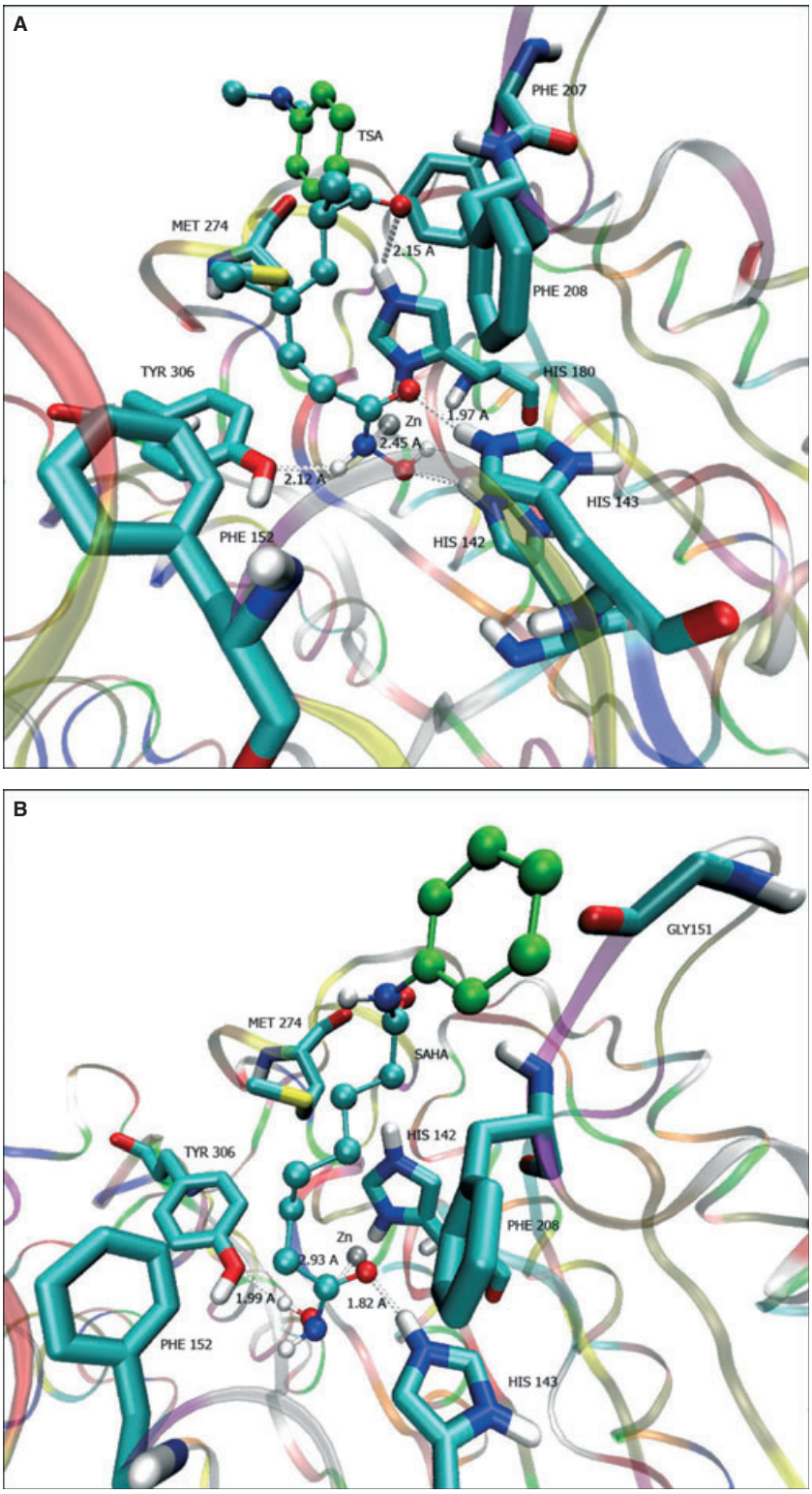

Figure 3: View of TSA (A), SAHA (B), in the active site cavity of HDAC8. The figures were generated by using VMD.

In recent years, phenolic compounds have attracted increasing attention for their potential as protection against oxidative stress and degenerative diseases (41). (*E*)-resveratrol, a phytoalexin, is one of the most promising agents among polyphenols. As the anti-carcinogenic (27) and anti-estrogenic (42) properties of (*E*)-resveratrol, which contains two functional moieties, namely, a *m*-hydroquinone moiety and a phenol moiety, on opposite rings, has come forward biological effects of this compound have been widely

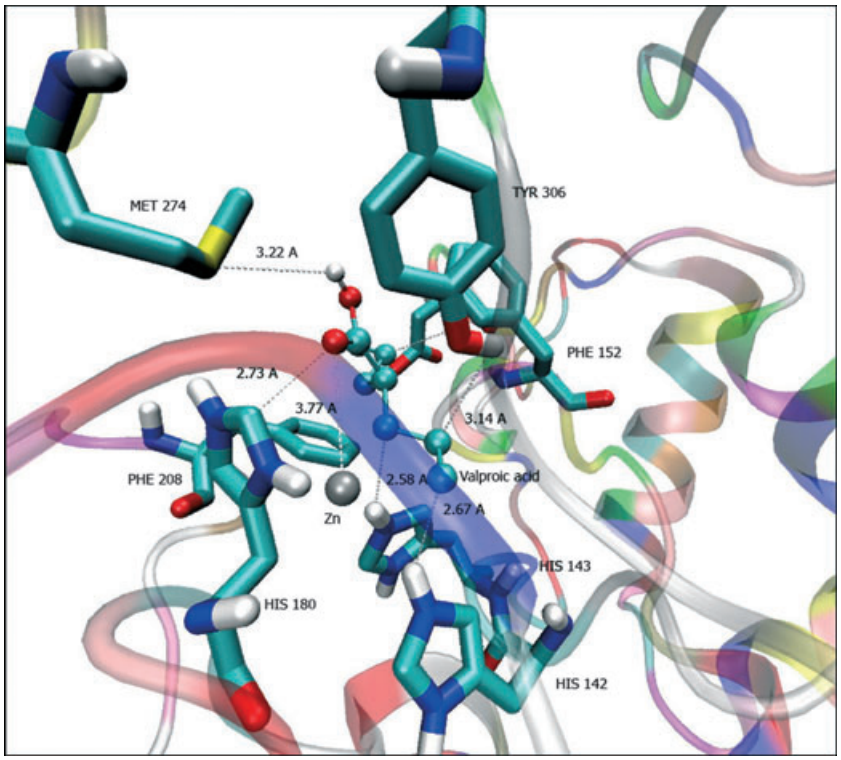

Figure 4: Interaction mode of valproic acid with HDAC8. The picture was generated using the VMD program.

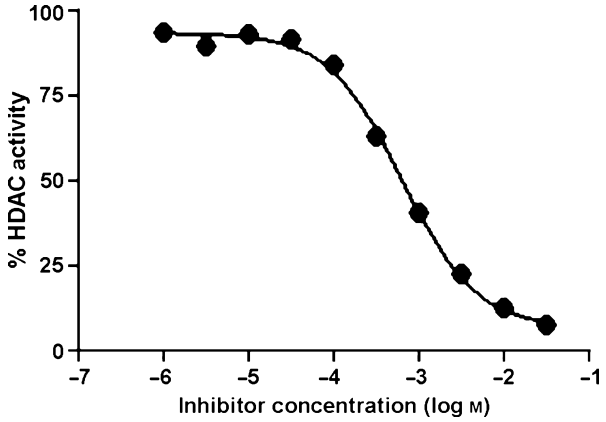

Figure 5: Half-maximum inhibition of total HDAC activity in HeLa nuclear extracts by (*E*)-resveratrol. The dose-response curve was determined by non-linear regression analysis. The top value of HDAC activity is set to 100%. Each concentration was performed in triplicate.

studied and reported in the literature (28,43,44). However, the HDAC inhibitor capacity of this compound in the treatment of degenerative diseases has not yet been explored. This study aimed to investigate the molecular docking and HDAC inhibition activity of (*E*)-resveratrol and its effect on *SMN2* transcriptional activation and/or modulation of the splicing pattern.

The invaluable data obtained by the molecular docking studies which allowed us to estimate the free energy of binding and binding mode are a promising tool for the discovery of new, active inhibitors useful as pharmacological agents in terms of the HDAC8 enzyme. In this study by using AutoDock molecular docking program, we showed that the order and the degree of inhibitions obtained for each compound computationally agreed with our experimental results. TSA and SAHA were studied by several groups experimentally and computationaly (45–47) and the results that they obtained are compatible with our results. We demonstrated that (*E*)-resveratrol shows the highest binding capacity towards the HDAC8 enzyme.

Histone deacetylases, 11 of which have been identified differ in their sequence homology, substrate specificity and requirement for cofactors (48). Within the three classes of HDACs, classes I and II HDACs are mediated by Zn-dependent mechanism, while class III HDACs (sirtuins) are mediated by an NAD-dependent mechanism. As the mechanism of the classes I and II HDACs is different from class III, a molecule such as resveratrol which was shown to activate SIRT1 by inducing a conformational change in the enzyme which permits tighter fluorophore binding in the context of the entire peptide substrate (49), has an inhibition activity towards class I HDACs (especially HDAC 8) via interaction with active site residues as His180, Phe208, Tyr306, Phe152, Gly151 and a zinc ion.

To obtain additional validations for molecular docking studies, HDAC inhibiton activity was determined. IC_{50} values of valproic acid and phenylbutyrate, which were effective in increasing *SMN* expression, were previously reported as 400 μM and 10 mM, respectively (50,51). We determined a dose-dependent HDAC inhibitor activity of (*E*)-resveratrol with an IC_{50} of 650 μM which was close to the IC_{50} of valproic acid. Histone deacetylase inhibitors differ in their potency and isoenzyme selectivity; therefore the

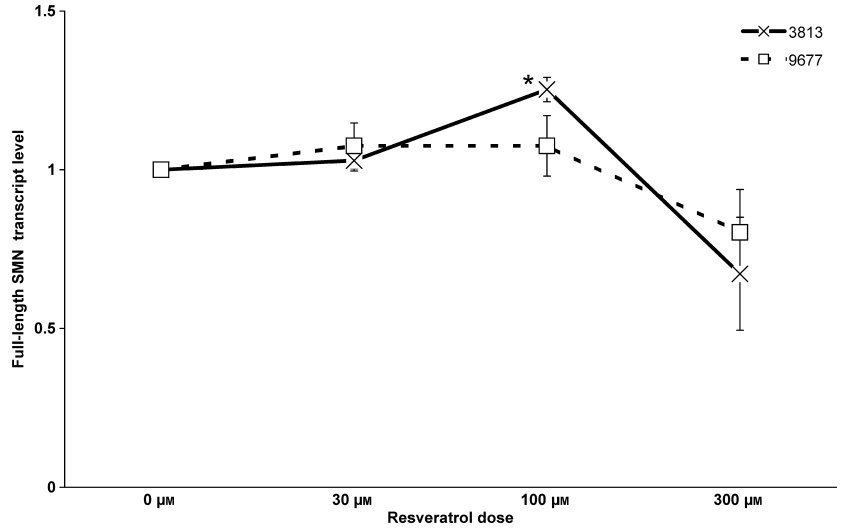

Figure 6: Effect of (*E*)-resveratrol treatment on levels of full-length *SMN* transcripts in two SMA type I fibroblast cell lines. The error bars represent standar deviation. Asterisks indicate significant differences in treated compared with untreated cells (*$p < 0.05$).

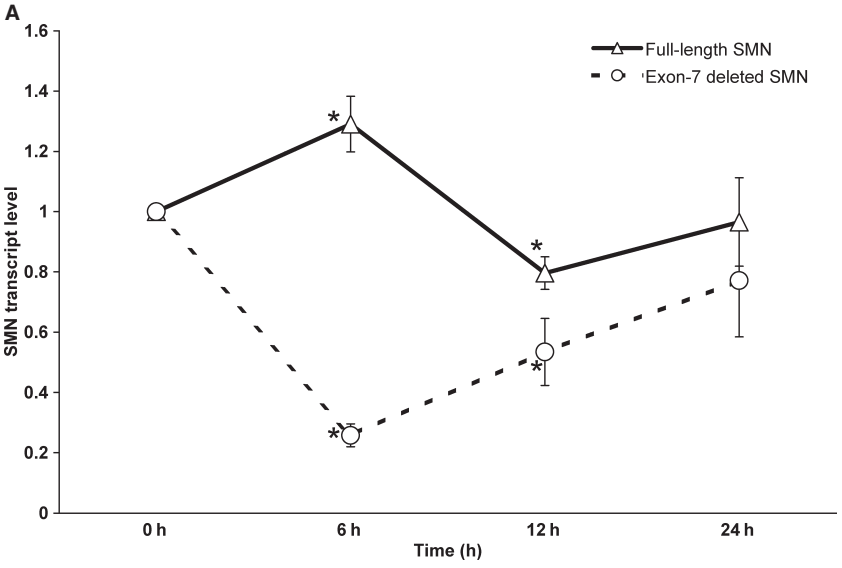

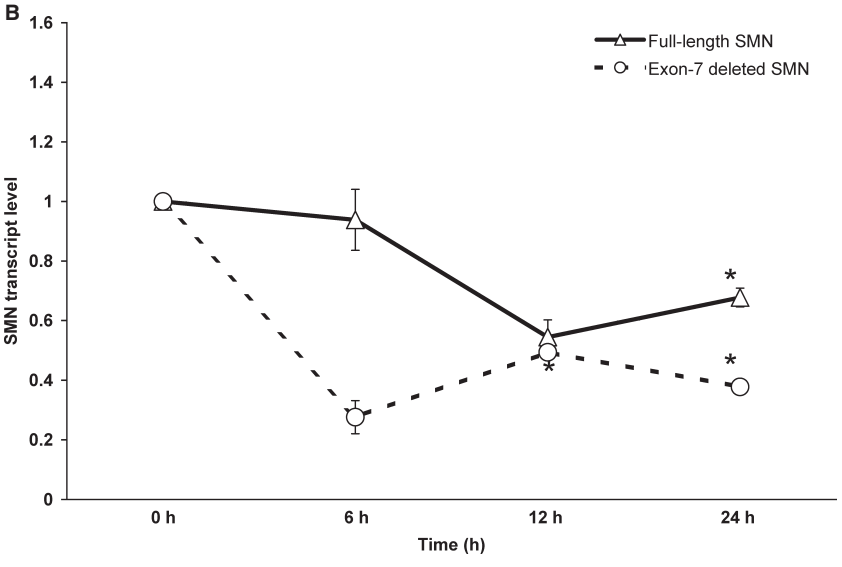

Figure 7: Effect of 100 μM (*E*)-resveratol treatment on full-length and exon 7–deleted *SMN2* transcript levels in the 3813 (A) and 9677 cell lines (B). The error bars represent standar deviation. Asterisks indicate significant differences in treated compared with untreated cells (*$p < 0.05$).

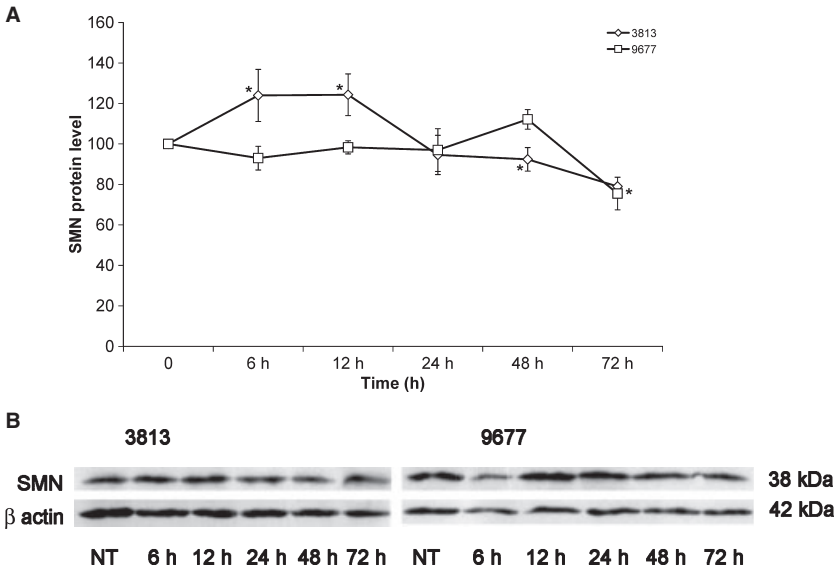

Figure 8: Effect of (*E*)-resveratrol treatment on SMN protein levels in two SMA type I fibroblast cell lines (A). The error bars represent standar deviation. Asterisks indicate significant differences in treated compared with untreated cells (*$p < 0.05$). Representative Western blot analysis of SMN protein (B).

half-maximum inhibition of total HDACs can be different among cell types because of tissue-specific expression. Previous studies have shown that valproic acid and sodium butyrate, which are relatively weak inhibitors, reduce HDAC2 levels whereas potent hydroxamic acid inhibitors like TSA and SAHA have no profound isoenzyme selectivity (52). On this point, to increase the specificity of inhibition, isoenzyme selectivity of (*E*)-resveratrol should be investigated in motor neurons because *SMN* expression is vital, especially for these cell types.

We showed that quantitative analysis of *SMN2* mRNA revealed increased full-length *SMN2* transcript levels after (*E*)-resveratrol treatment. A 1.3-fold increase in the full-length *SMN2* mRNA and protein level was determined at 100 μM (*E*)-resveratrol after 6 h of treatment in 3813 cell line. Similar to our results, in a recent study it was demonstrated that (*E*)-resveratrol stimulated the production of full-length *SMN2* RNA and protein in the same line (53). We also analyzed the effect of (*E*)-resveratrol in 9677 cell line and found no increase in the full-length *SMN2* mRNA level. These results indicate that response to (*E*)-resveratrol treatment is variable among cell lines. The causes of the variability in response to (*E*)-resveratrol treatment are unknown but may be related to the copy number of *SMN2* genes. But in this case, although the two cell lines have two *SMN2* copies, they responded to (*E*)-resveratrol treatment regardless of copy number. Unknown factors such as modifier genes or interindividual differences in drug response caused by genetic polymorphisms in genes encoding drug-metabolizing enzymes, drug transporters, drug targets may also contribute to the variability in both cell lines. The detection of a slight increase in the SMN protein at 48 h in 9677 line may suggest that this is a low responding cell line and repetitive administration of (*E*)-resveratrol may enhance the protein level. The decrease in the level of the SMN protein below baseline may be due to reduction of cell viability and cytotoxicity (54). We also showed that *SMN2*Δ7 transcripts decreased as full-length *SMN2* transcripts increased in 3813 cell line. This may suggest reversion of the splicing pattern of *SMN2* mRNA by (*E*)-resveratrol treatment and could be explained by increased expression of splicing factors that promote *SMN2* exon 7 inclusion. Further experiments are necessary to investigate the mode of action of (*E*)-resveratrol on *SMN* gene expression. Although TSA is a well-known and highly potent HDAC inhibitor, it has not yet been developed for SMA clinical trials. To monitor specificity, 3813 cell line was treated with 2.5–50 nM TSA for 6 h and twofold increase in the full-length *SMN2* mRNA level was observed (data not shown).

Among our candidate prodrug library, (*E*)-resveratrol was found to have a high HDAC inhibitor activity. This novel activity, which is to inhibit HDACs at a micromolar dose was demonstrated by both *in silico* and experimental-based analysis. Modifications of (*E*)-resveratrol may increase the possibility of developing more potent candidates that are promising in the treatment of SMA.

Conclusions and Future Directions

In this study, we found that (*E*)-resveratrol, which is one of the most promising agents among polyphenols, shows the highest binding capacity toward HDAC8 enzyme than known HDAC inhibitors and has a dose-dependent HDAC inhibitor activity. Our findings reveal that (*E*)-resveratrol increases the level of full-length *SMN2* mRNA and protein in SMA type I fibroblast cell line. On the basis of these observations, future studies will aim rational design of novel selective and potent HDAC inhibitors for the treatment of SMA.

Acknowledgments

This work was supported by the Scientific and Technological Research Council of Turkey, Research Project No: 105G014.

References

1. Pearn J. (1980) Classification of spinal muscular atrophies. Lancet;1:919–922.
2. Crawford T.O., Pardo C.A. (1996) The neurobiology of childhood spinal muscular atrophy. Neurobiol Dis;3:97–110.
3. Lefebvre S., Bürglen L., Reboullet S., Clermont O., Burlet P., Viollet L., Benichou B. *et al.* (1995) Identification and characterization of a spinal muscular atrophy determining gene. Cell;80:155–165.
4. Erdem H., Pehlivan S., Topaloğlu H., Ozgüç M. (1999) Deletion analysis in Turkish patients with spinal muscular atrophy. Brain Dev;21:86–89.
5. Rodrigues N.R., Owen N., Talbot K., Ignatius J., Dubowitz V., Davies K.E. (1995) Deletions in the survival motor neuron gene on 5q13 in autosomal recessive spinal muscular atrophy. Hum Mol Genet;4:631–634.
6. Burghes A.H. (1997) When is a deletion not a deletion? When it is converted Am J Hum Genet;61:9–15.
7. Lorson C.L., Hahnen E., Androphy E.J., Wirth B. (1999) A single nucleotide in the SMN gene regulates splicing and is responsible for spinal muscular atrophy. Proc Natl Acad Sci USA;96:6307–6311.
8. Lefebvre S., Burlet P., Liu Q., Bertrandy S., Clermont O., Munnich A., Dreyfuss G., Melki J. (1997) Correlation between severity and SMN protein level in spinal muscular atrophy. Nat Genet;16:265–269.
9. Pellizzoni L., Kataoka N., Charroux B., Dreyfuss G. (1998) A novel function for SMN, the spinal muscular atrophy disease gene product, in pre-mRNA splicing. Cell;95:615–624.
10. Narayanan U., Achsel T., Lührmann R., Matera A.G. (2004) Coupled in vitro import of U snRNPs and SMN, the spinal muscular atrophy protein. Mol Cell;16:223–234.
11. Zhang H., Xing L., Rossoll W., Wichterle H., Singer R.H., Bassell G.J. (2006) Multiprotein complexes of the survival of motor neuron protein SMN with Gemins traffic to neuronal processes and growth cones of motor neurons. J Neurosci;26:8622–8632.
12. Monani U.R., Coovert D.D., Burghes A.H. (2000) Animal models of spinal muscular atrophy. Hum Mol Genet;9:2451–2457.
13. Chang J.G., Hsieh-Li H.M., Jong Y.J., Wang N.M., Tsai C.H., Li H. (2001) Treatment of spinal muscular atrophy by sodium butyrate. Proc Natl Acad Sci USA;98:9808–9813.
14. Andreassi C., Angelozzi C., Tiziano F.D., Vitali T., De Vincenzi E., Boninsegna A., Villanova M., Bertini E., Pini A., Neri G., Brahe C. (2004) Phenylbutyrate increases SMN expression in vitro: relevance for treatment of spinal muscular atrophy. Eur J Hum Genet;12:59–65.
15. Sumner C.J., Huynh T.N., Markowitz J.A., Perhac J.S., Hill B., Coovert D.D., Schussler K., Chen X., Jarecki J., Burghes A.H., Taylor J.P., Fischbeck K.H. (2003) Valproic acid increases SMN levels in spinal muscular atrophy patient cells. Ann Neurol;54:647–654.
16. Brichta L., Hofmann Y., Hahnen E., Siebzehnrubl F.A., Raschke H., Blumcke I., Eyupoglu I.Y., Wirth B. (2003) Valproic acid increases the SMN2 protein level: a well-known drug as a potential therapy for spinal muscular atrophy. Hum Mol Genet;12:2481–2489.
17. Riessland M., Brichta L., Hahnen E., Wirth B. (2006) The benzamide M344, a novel histone deacetylase inhibitor, significantly increases SMN2 RNA/protein levels in spinal muscular atrophy cells. Hum Genet;120:101–110.
18. Avila A.M., Burnett B.G., Taye A.A., Gabanella F., Knight M.A., Hartenstein P., Cizman Z., Di Prospero N.A., Pellizzoni L., Fischbeck K.H., Sumner C.J. (2007) Trichostatin A increases SMN expression and survival in a mouse model of spinal muscular atrophy. J Clin Invest;117:659–671.
19. Hahnen E., Eyüpoglu I.Y., Brichta L., Haastert K., Tränkle C., Siebzehnrübl F.A., Riessland M., Hölker I., Claus P., Romstöck J., Buslei R., Wirth B., Blümcke I. (2006) In vitro and ex vivo evaluation of second-generation histone deacetylase inhibitors for the treatment of spinal muscular atrophy. J Neurochem;98:193–202.
20. Kelly W.K., O'Connor O.A., Marks P.A. (2002) Histone deacetylase inhibitors: from target to clinical trials. Expert Opin Invest Drugs;11:1695–1713.
21. Marks P.A., Richon V.M., Miller T., Kelly W.K. (2004) Histone deacetylase inhibitors. Adv Cancer Res;91:137–168.
22. Somoza J.R., Skene R.J., Katz B.A., Mol C., Ho J.D., Jennings A.J., Luong C. *et al.* (2004) Structural snapshots of human HDAC8 provide insights into the class I histone deacetylases. Structure;12:1325–1334.
23. Mercuri E., Bertini E., Messina S., Solari A., D'Amico A., Angelozzi C., Batini R. *et al.* (2007) Randomized, double-blind, placebo-controlled trial of phenylbutyrate in spinal muscular atrophy. Neurology;68:51–55.
24. Brichta L., Holker I., Haug K., Klockgether T., Wirth B. (2006) In vivo activation of SMN in spinal muscular atrophy carriers and patients treated with valproate. Ann Neurol;59:970–975.
25. Weihl C.C., Connolly A.M., Pestronk A. (2006) Valproate may improve strength and function in patients with type III/IV spinal muscle atrophy. Neurology;67:500–501.
26. Arts I.C., Hollman P.C. (2005) Polyphenols and disease risk in epidemiologic studies. Am J Clin Nutr;81:317S–325S.
27. Jang M., Cai L., Udeani G.O., Slowing K.V., Thomas C.F., Beecher C.W., Fong H.H., Farnsworth N.R., Kinghorn A.D., Mehta R.G., Moon R.C., Pezzuto J.M. (1997) Cancer chemopreventive activity of resveratrol, a natural product derived from grapes. Science;275:218–220.
28. Frémont L. (2000) Biological effects of resveratrol. Life Sci;66:663–673.
29. Aziz M.H., Kumar R., Ahmad N. (2003) Cancer chemoprevention by resveratrol: in vitro and in vivo studies and the underlying mechanisms. Int J Oncol;23:17–28.
30. Rubiolo J.A., Mithieux G., Vega F.V. (2008) Resveratrol protects primary rat hepatocytes against oxidative stress damage: activation of the Nrf2 transcription factor and augmented activities of antioxidant enzymes. Eur J Pharmacol;591:66–72.
31. Hayashi M., Araki S., Arai N., Kumada S., Itoh M., Tamagawa K., Oda M., Morimatsu Y. (2002) Oxidative stress and disturbed glutamate transport in spinal muscular atrophy. Brain Dev;24:770–775.
32. Sanner M.F. (1999) A programming language for software integration and development. J Mol Graph Model;17:57–61.
33. Gasteiger J., Marsili M. (1980) Iterative partial equalization of orbital electronegativity – a rapid access to atomic charges. Tetrahedron;36:3219–3228.
34. Morris G.M., Goodsell D.S., Halliday R.S., Huey R., Hart W.E., Belew R.K., Olson A.J. (1998) Automated docking using a

Lamarckian genetic algorithm and an empirical binding free energy function. J Comput Chem;19:1639–1662.
35. Huey R., Morris G.M., Olson A.J., Goodsel D.S. (2007) A semi-empirical free energy force field with charge-based desolvation. J Comput Chem;28:1145–1152.
36. Humphrey W., Dalke A., Schulten K. (1996) VMD: visual molecular dynamics. J Mol Graph;14:33–38.
37. Sumner C.J. (2006) Therapeutics development for spinal muscular atrophy. NeuroRx;3:235–245.
38. Glaser K.B., Staver M.J., Waring J.F., Stender J., Ulrich R.G., Davidsen S.K. (2003) Gene expression profiling of multiple histone deacetylase (HDAC) inhibitors: defining a common gene set produced by HDAC inhibition in T24 and MDA carcinoma cell lines. Mol Cancer Ther;2:151–163.
39. Cartegni L., Krainer A.R. (2002) Disruption of an SF2/ASF-dependent exonic splicing enhancer in SMN2 causes spinal muscular atrophy in the absence of SMN1. Nat Genet;30:377–384.
40. Kernochan L.E., Russo M.L., Woodling N.S., Huynh T.N., Avila A.M., Fischbeck K.H., Sumner C.J. (2005) The role of histone acetylation in SMN gene expression. Hum Mol Genet;14:1171–1182.
41. Ramassamy C. (2006) Emerging role of polyphenolic compounds in the treatment of neurodegenerative diseases: a review of their intracellular targets. Eur J Pharmacol;545:51–64.
42. Gehm B.D., McAndrews J.M., Chien P.Y., Jameson J.L. (1997) Resveratrol, a polyphenolic compound found in grapes and wine, is an agonist for the estrogen receptor. Proc Natl Acad Sci USA;94:14138–14143.
43. Soleas G.J., Diamandis E.P., Goldberg D.M. (1997) Resveratrol: a molecule whose time has come? And gone? Clin Biochem;30:91–113.
44. Bhat K.P.L., Kosmeder J.W., Pezzuto J.M. (2001) Biological effects of resveratrol. Antioxid Redox Signal;3:1041–1064.
45. Wang D.F., Helquist P., Wiech N.L., Wiest O. (2005) Toward selective histone deacetylase inhibitor design: homology modeling, docking studies, and molecular dynamics simulations of human class I histone deacetylases. J Med Chem;48:6936–6947.
46. Wang D.F., Wiest O., Helquist P., Lan-Hargest H.Y., Wiech N.L. (2004) On the function of the 14 A long internal cavity of histone deacetylase-like protein: implications for the design of histone deacetylase inhibitors. J Med Chem;47:3409–3417.
47. Krennhrubec K., Marshall B.L., Hedglin M., Verdin E., Ulrich S.M. (2007) Design and evaluation of 'Linkerless' hydroxamic acids as selective HDAC8 inhibitors. Bioorg Med Chem Lett;15:2874–2878.
48. Gray S.G., Ekstrom T.J. (2001) The human histone deacetylase family. Exp Cell Res;262:75–83.
49. Bora M.T., Smith B.C., Denu J.M. (2005) Mechanism of human SIRT1 activation by resveratrol. J Biol Chem;280:17187–17195.
50. Deubzer H., Busche B., Ronndahl G., Eikel D., Michaelis M., Cinatl J., Schulze S., Naud H., Witt O. (2006) Novel valproic acid derivatives with potent differentiation-inducing activity in myeloid leukemia cells. Leukemia Res;30:1167–1175.
51. Gardian G., Browne S.E., Choi D.K., Klivenyi P., Gregorio J., Kubilus J.K., Ryu H., Langley B., Ratan R.R., Ferrante R.J., Beal M.F. (2005) Neuroprotective effects of phenylbutyrate in the N171-82Q transgenic mouse model of Huntington's disease. J Biol Chem;280:556–563.
52. Hahnen E., Hauke J., Tränkle C., Eyüpoglu I.Y., Wirth B., Blümcke I. (2008) Histone deacetylase inhibitors: possible implications for neurodegenerative disorders. Expert Opin Investig Drugs;17:169–184.
53. Sakla M.S., Lorson C.L. (2008) Induction of full-length survival motor neuron by polyphenol botanical compounds. Hum Genet;122:635–643.
54. Joe A.K., Liu H., Suzui M., Vural M.E., Xiao D., Weinstein I.B. (2002) Resveratrol induces growth inhibition, S-phase arrest, apoptosis, and changes in biomarker expression in several human cancer cell lines. Clin Cancer Res;8:893–903.

Note

[a]SPARTAN'02, Irvine, CA, USA: Wavefunction Inc.